

*Supplementary information for*

**Bi<sub>2</sub>O<sub>2</sub>CO<sub>3</sub>/Bi<sub>2</sub>O<sub>3</sub> Z-scheme photocatalyst with oxygen vacancies  
and Bi for enhanced visible-light photocatalytic degradation of  
tetracycline**

Shoubin Huang<sup>a</sup>, Yuliang Wu<sup>b</sup>, Qianxin Zhang<sup>c</sup>, Xiaoyu Jin<sup>a</sup>, Daguang Li<sup>a</sup>,  
Haijin Liu<sup>d</sup>, Ping Chen<sup>a</sup>, Wenying Lv<sup>a</sup> and Guoguang Liu<sup>a\*</sup>.

<sup>a</sup> *School of Environmental Science and Engineering, Guangdong University of  
Technology, Guangzhou, 510006, China*

<sup>b</sup> *Shenzhen Key Laboratory of Organic Pollution Prevention and Control,  
Environmental Science and Engineering Research Center, Harbin Institute of  
Technology, Shenzhen, Guangdong 518055, China*

<sup>c</sup> *School of Environment, Tsinghua University, Beijing, 100084, China*

<sup>d</sup> *Key Laboratory for Yellow River and Huaihe River Water Environment and  
Pollution Control, School of Environment, Henan Normal University, Xinxiang,  
453007, China*

\* Corresponding Author: Guoguang Liu, E-mail: [liugg615@163.com](mailto:liugg615@163.com), Phone: +86-20-  
39322547, Fax: +86-20-39322548

---

## Contents

Text S1. Material synthesis .....	4
2.1.1. Synthesis of BOC and BO.....	4
2.1.2. Synthesis of BOC/BO materials.....	4
2.1.3. Synthesis of Bi-BOC/BO-OVs materials.....	4
Text S2. Determination of concentration of TC.....	5
Text S3. Characterization.....	5
Text S4. Recycling procedure .....	6
Table S1. C and O and Bi contents in as-prepared samples according to XPS results .....	7
Table S2. XPS elemental analysis of Bi 4f for Bi-BOC/BO-OVs.....	7
Table S3. Fluorescence decay parameters of BOC, BO, BOC/BO and Bi-BOC/BO-OVs fit for the decay.....	7
Table S4. Comparison of results (degradation of TC) from our work with other works.....	8
Table S5. Production costs of Bi-BOC/BO-OVs (laboratory level). The price of energy was 0.79 ¥/kW·h, price of $\text{Bi}(\text{NO}_3)_3 \cdot 5\text{H}_2\text{O}$ was 312.84 ¥/kg, price of $\text{C}_6\text{H}_8\text{O}_7 \cdot \text{H}_2\text{O}$ was 109.8 ¥/kg, price of $\text{HNO}_3$ was 141.3 ¥/L, price of NaOH was 118.44 ¥/kg, prices correspond to the Chinese market. ....	9
Table S6. The rhizomes length of soybean seedlings under the solution of different concentrations of catalyst, before reaction (A) and after 60 min irradiation (B). .....	10

---

Table S7. Chemical structure of the TC and its by-products. ....	10
Table S8. Scavengers used, RSs quenched, and photocatalytic efficiency with quenched reactive species during the photocatalytic TC degradation process. ....	12
Fig S1. (a) XRD spectrum and (b) UV-vis DRS spectra of Bi-BOC/BO-OVs system calcined at different temperatures. ....	13
Fig. S2. (a) Ex-situ/ in-situ irradiated XPS spectra of C1s. (b) High-resolution XPS spectra of Bi 4f. (c) FT-IR spectrum and (d) Raman spectra of BOC, BO, and Bi-BOC/BO-OVs. ....	14
Fig S3. Adsorption for TC in the darkness of (a) different samples, (b) different photocatalyst concentrations and (c) different pH of Bi-BOC/BO-OVs. (d) Self-degradation of TC at different pH without catalyst. ....	14
Fig S4. (a) Zeta potential of Bi-BOC/BO-OVs. (b) Species distribution of tetracycline under different pH. ....	15
Fig S5. Leakage of Bi ions in the Bi-BOC/BO-OVs system. ....	15
Fig S6. The mineralization of tetracycline during Bi-BOC/BO-OVs photocatalytic degradation process under visible light. ....	16
Fig S7. Fragment chart analyses of the UHPLC-HRMS secondary ion mass spectrometry of the TC and its by-products. ....	21

---

## Texts

### Text S1. Material synthesis

#### 2.1.1. Synthesis of BOC and BO

The bismuth subcarbonate (BOC) nanospheres were synthesized according to the synthesis procedure reported elsewhere, with appropriate modification of the synthesis conditions.<sup>1</sup> In detail, 0.97 g of bismuth nitrate pentahydrate ( $\text{Bi}(\text{NO}_3)_3 \cdot 5\text{H}_2\text{O}$ ) was dissolved in 10 mL of 1 M nitric acid ( $\text{HNO}_3$ ), and 0.31 g citric acid monohydrate was then introduced into the solution. The pH of the mixed solution was adjusted to 4.2 with the dropwise addition of sodium hydroxide (NaOH) aqueous solution. The mixed solution was then transferred to a sealed 100 mL Teflon autoclave and heated to 180 °C for 24 h. After naturally cooled to room temperature, the synthetic samples were washed 4 times with deionized water and ethanol in turn and dried under vacuum overnight at 60 °C to obtain the BOC precursor powders. The BOC precursor powder was calcined in a muffle furnace at 350 °C for 2 h to obtain pure BO materials.

#### 2.1.2. Synthesis of BOC/BO materials

For comparison, the BOC precursor powder was calcined in a muffle furnace at 320 °C for 2 h to obtain the BOC/BO materials.

#### 2.1.3. Synthesis of Bi-BOC/BO-OVs materials

The Bi-BOC/BO-OVs materials were synthesized by BOC precursor powders, which were calcined at temperatures in the range of 280°C~380 °C (with 20 °C intervals) for 2 h under  $\text{N}_2$  atmosphere.

---

**Text S2. Determination of concentration of TC.**

The concentration of residual TC was detected by high performance liquid chromatography (HPLC, SHIMADZU LC16, Japan). The temperature of Zorbax Eclipse XDB C18 reverse-phase column (4.6×150mm, Agilent, USA) was maintained at 35.0 °C and the detection wavelength of the UV detector was 355 nm. The isocratic mobile phase was made up of 30% methanol and 70% water (with 0.2% formic acid) with a flow rate of 1.0 mL min<sup>-1</sup>.

**Text S3. Characterization**

The morphologies of the as-prepared photocatalysts were obtained using scanning electron microscopy (SEM, Hitachi S4800) and transmission electron microscopy (TEM, JEM-2100HR). The specific surfaces area and distribution of pore size was estimated by the Brunauer-Emmett-Teller (BET) method using an ASAP 2020 PLUS HD88 analyzer. Powder X-ray diffraction (XRD) patterns were recorded on a Bruker D8 ADVANCE diffractometer with a Cu K $\alpha$  radiation source ( $\lambda = 0.15418$  nm). Fourier transform infrared (FT-IR) measurements were achieved with a Thermo Fisher Nicolet IS50 spectrophotometer. Micro Confocal Raman spectroscopy was measured by HORIBA Jobin-Yvon-LabRAM HR Evolution. X-ray photoelectron spectroscopy (XPS) characterization was accomplished using a Thermo Fisher Scientific ESCALAB 250Xi spectrometer with an Al K $\alpha$  source. Room temperature EPR spectroscopy was performed on probe unpaired electrons of products using an ESR JES-FA200 spectrometer. UV-vis diffuse reflectance spectra (DRS) were obtained via a SHIMADZU UV-2450 spectrophotometer. Photoluminescence (PL)

---

spectra and transient photoluminescence decay (TRPL) spectra were collected using a HORIBA FluoroMax-4 Fluor-spectrophotometer and a FLS 980 fluorescence lifetime spectrophotometer, respectively. The photoelectrochemical properties of the samples were recorded on an electrochemical workstation (Multi Autolab/204, Metrohm Autolab B.V.) using a Pt wire electrode and saturated calomel electrodes (SCE) as the counter electrode and reference electrode, respectively. A 0.1 M Na<sub>2</sub>SO<sub>4</sub> aqueous solution was used as the electrolyte. The TOC removal ratio of the as-prepared photocatalysts was detected using a TOC-VCPH analyzer (SHIMADZU, Japan). The content of bismuth in the solution is detected by inductively coupled plasma-mass spectrometry (ICP-MS, Agilent 700).

#### **Text S4. Recycling procedure**

In the cyclic experiment, we established 1 experimental group and 11 control groups to ensure that the amount of catalyst and TC in each experiment remained same. Specifically, the initial experimental conditions were as follows: 240 mg catalyst was added to 600 mL of the TC solution. Once the suspension reached adsorption-desorption equilibrium, the suspended liquid was evenly transferred to 12 quartz tubes for photolytic degradation experiments. The circulating sample was separated by centrifugation and washed with ultrapure water and ethanol for 4 times in turn. Subsequently, the powder was dried in vacuum oven at 60 °C overnight, which was utilized for subsequent degradation experiments. During the cycling experiments, following the decrease of the photocatalyst mass, the volumes of the reaction solutions were correspondingly altered to maintain an invariable

---

photocatalyst concentration.

#### **Text S5. Determination of RSs**

Reactive oxidative species generated during tetracycline degradation were determined by performing scavenger-quenching experiments. Specifically, isopropanol (IPA), methyl alcohol (MeOH), histidine (His) and 4-hydroxy-2,2,6,6-tetramethylpiperidinyloxy (TEMP) were employed as hydroxyl radical ( $\cdot\text{OH}$ ) scavengers, photogenerated holes ( $h^+$ ), singlet oxygen ( $^1\text{O}_2$ ) and superoxide radicals ( $\text{O}_2^{\cdot-}$ ), respectively. Scavengers were added to the samples prior to irradiation. Subsequently, each sample suspension was collected for further analysis.

Electron spin resonance (ESR) was used for further direct detection of reactive species. A solution of 0.4 mg/L catalyst and 100 mM capture agent was irradiated under visible light. Specifically,  $\cdot\text{OH}$  were detected in DMPO aqueous solution,  $\text{O}_2^{\cdot-}$  were detected in DMPO methanol solution, and  $^1\text{O}_2$  were detected in TEMP aqueous solution. Subsequently, DMPO- $\cdot\text{OH}$ , DMPO- $\text{O}_2^{\cdot-}$ , and TEMP- $^1\text{O}_2$  signal was measured at different times. Electron spin resonance detection conditions are as follows. Microwave frequency: 9224.637 MHz, power: 0.998 mW, phase: 292, coupling: 242, scanning width: 5 mT, scanning time: 1 min, center field: 329.400 mT.

#### **Text S6. Toxicity test of mung bean**

The toxicity of the materials and tetracycline before and after the degradation was investigated by the toxicity test of mung bean. A number of dry and plump mung beans with a mass range between 0.68 - 0.73 g were selected for experiment. Before the experiment, the mung beans were soaked in ultrapure water at a temperature of

---

about 30 °C for 3 hours for germination pretreatment. Subsequently, each 5 mung beans were placed in a 20 mL clear headspace vial. 2 mL the Bi-BOC/BO-OVs solutions with concentrations of 0, 10, 20, 40, 60, 100 mg/L and the reaction solution before irradiation and after irradiation for 60 min were added to the headspace vials for cultivation. The culture environment was carried out in a constant temperature incubator at 27 °C, and the nutrient solution was supplemented every 12 hours. After 120 h cultivation, all the germinated mung beans were taken out and the length of the main body above the root was measured with a ruler.



---

## Tables

**Table S1. C and O and Bi contents in as-prepared samples according to XPS results**

Samples	C	O	Bi	C/O/Bi	$\Delta O/\Delta C$
BOC	65.47%	27.51%	7.02%	9.33/3.92/1	3/1
Bi-BOC/BO-OVs	66.54%	26.26%	7.2%	9.24/3.65/1	

**Table S2. XPS elemental analysis of Bi 4f for Bi-BOC/BO-OVs.**

Binding energy and type of bonding	164.1 eV Bi <sup>3+</sup>	162.8 eV Bi <sup>0</sup>	158.8 eV Bi <sup>3+</sup>	157.4 eV Bi <sup>0</sup>
percentage composition	42.4%	0.8%	53.3%	3.5%
n				

According to the area ratio of the diffraction peaks in Bi 4f, the percentage content of different valence states of Bi was calculated. The sum of 4f<sub>7/2</sub> (164.1 eV) and 4f<sub>5/2</sub> (158.8 eV) is 95.7%, which means that the content of Bi<sup>3+</sup> in the bismuth element accounts for 95.7%, and the content of Bi<sup>0</sup> is 4.3%. This is consistent with what others have reported.<sup>2</sup> The diffraction peaks of Bi<sup>0</sup> proved the existence of metallic Bi.

**Table S3. Fluorescence decay parameters of BOC, BO, BOC/BO and Bi-BOC/BO-OVs fit for the decay.**

Sample	$\tau_1$ (ns)	$B_1$	$\tau_2$ (ns)	$B_2$	$\tau_3$ (ns)	$B_3$	$\tau$ (ns)
BOC	0.0525	1.357	1.7693	0.079	6.7295	0.015	2.982
BO	0.1194	0.776	1.6274	0.107	7.5375	0.015	3.019
BOC/BO	0.1711	0.960	2.0137	0.039	15.7999	0.002	2.498
Bi-BOC/BO-OVs	0.1783	0.216	1.4042	0.015	5.7347	0.002	1.439

**Table S4. Comparison of results (degradation of TC) from our work with other works.**

Photocatalyst with dose	Morphology	Light source and irradiation time	Photocatalytic performance	Ref
<b>Bi<sub>2</sub>O<sub>2</sub>CO<sub>3</sub></b> (10mg in 40 mL drug solution)	Flower-like spherical	Visible light irradiation 180 min	89.4% degradation of TC (10 mg/L)	1
<b>OVs-Bi<sub>2</sub>O<sub>2</sub>CO<sub>3</sub></b> (50mg in 50 mL drug solution)	Irregular nanoplates	Visible light irradiation 300 min	50% degradation of TC (10 mg/L)	3
<b>OVs-BiOCl/Bi<sub>2</sub>O<sub>2</sub>CO<sub>3</sub></b> (25mg in 50 mL drug solution)	Pinecone-like	Visible light irradiation 200 min	90% degradation of TC (20 mg/L)	4

---

<b>CeO<sub>2</sub>/Bi<sub>2</sub>O<sub>2</sub>CO<sub>3</sub></b> (35 mg in 100 mL drug solution)	Spherical	Visible light	79.5% degradation	5
	Flower	irradiation 90 min	of TC (20 mg/L)	
<b>β-Bi<sub>2</sub>O<sub>3</sub>/Bi<sub>2</sub>O<sub>2</sub>CO<sub>3</sub></b> (100 mg in 100 mL drug solution)	Flower-like	Simulated sunlight	98.8% degradation	6
	hierarchical	irradiation 60min	of TC (30 mg/L)	
<b>g-C<sub>3</sub>N<sub>4</sub>/Bi<sub>2</sub>O<sub>2</sub>CO<sub>3</sub></b> (20mg in 40 mL drug solution)	Irregular brick	Simulated sunlight	~95% degradation	7
		irradiation 360min	of TC (20 mg/L)	
<b>Ag<sub>3</sub>VO<sub>4</sub>/Bi<sub>2</sub>O<sub>2</sub>CO<sub>3</sub></b> (40mg in 80 mL drug solution)	Flower-like	Visible light	83.7% degradation	8
	microspheres	irradiation 180 min	of TC (20 mg/L)	
<b>Bi-Bi<sub>2</sub>O<sub>2</sub>CO<sub>3</sub>/</b>				
<b>Bi<sub>2</sub>O<sub>3</sub>-OVs</b> (20mg in 50 mL drug solution)	Porous	Visible light	92.9% degradation	Our work
	microsphere	irradiation 60 min	of TC (15 mg/L)	

---

**Table S5. Production costs of Bi-BOC/BO-OVs (laboratory level). The price of energy was 0.79 ¥/kW·h, price of  $\text{Bi}(\text{NO}_3)_3 \cdot 5\text{H}_2\text{O}$  was 312.84 ¥/kg, price of  $\text{C}_6\text{H}_8\text{O}_7 \cdot \text{H}_2\text{O}$  was 109.8 ¥/kg, price of  $\text{HNO}_3$  was 141.3 ¥/L, price of NaOH was 118.44 ¥/kg, prices correspond to the Chinese market.**

Sample	Chemicals Cost (¥/kg)	Energy Cost (¥/kg)	Total Cost (¥/kg)
Bi-BOC/BO-OVs	1103.21	31.64	1134.85

As shown in Table S5, We calculated the cost required to manufacture 1kg product based on the price in the Chinese market (laboratory level). In the calculation, the yield of 65.51% was taken according to the actual situation. It can be seen that nitric acid takes a large proportion of the total cost. In the work, the role of nitric acid is to help the hydrolysis of  $\text{Bi}(\text{NO}_3)_3 \cdot 5\text{H}_2\text{O}$  and adjust the pH for morphology control. Owing to morphology control is not the main reason for the improvement of the catalytic efficiency of Bi-BOC/BO-OVs, the amount of nitric acid can be appropriately reduced to reduce production costs in the actual production process. Furthermore, considering the large amount used in the real environment, the actual production cost will be further reduced.

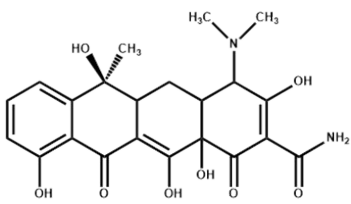
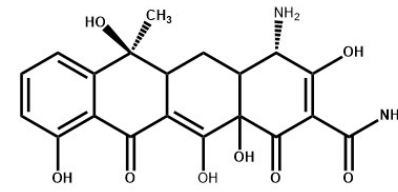
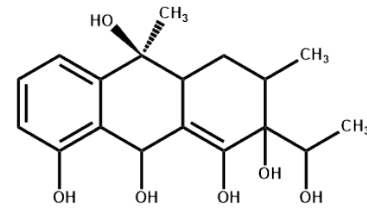
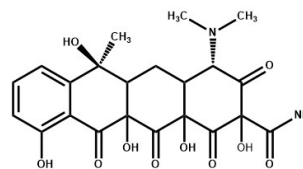
**Table S6. The rhizomes length of soybean seedlings under the solution of different concentrations of catalyst, before reation (A) and after 60 min irradiation (B).**

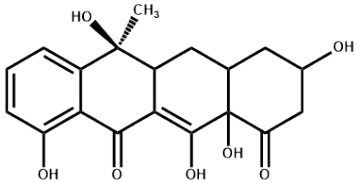
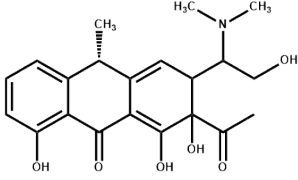
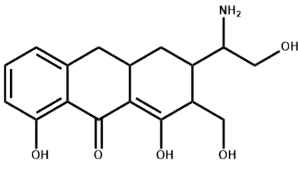
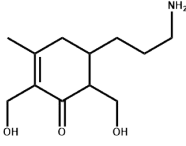
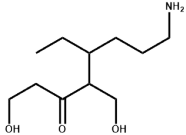
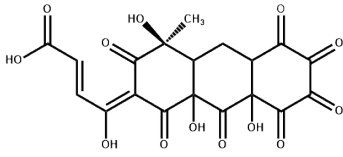
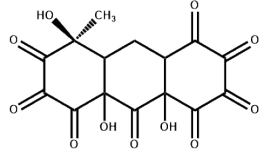
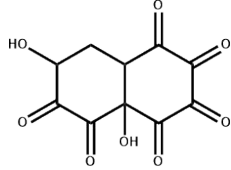
	0	10	20	40	60	100	A	B
<b>Rhizomes Length (mm)</b>	143.18	143.52	144.13	143.63	142.78	141.85	137.06	145.46

**Table S7. The relationship of catalyst concentration and rhizomes by one-way ANOVA.**

Catalyst concentration (mg/L)	n	$\bar{x} \pm s$	F	P
0	5	143.17±0.75	3.910	0.01<0.05
10	5	143.52±0.43		
20	5	144.13±0.61		
40	5	143.63±0.53		
60	5	142.78±0.66		
100	5	141.84±0.94		

**Table S8. Chemical structure of the TC and its by-products.**

Compound	Molecular weight	Retention time (min)	Chemical structure
TC	444		
P1	416	11.28	
P2	337	18.72	
P3	476	17.89	

P4	360	18.69	
P5	387	8.82	
P6	318	17.17	
P7	226	15.13	
P8	217	10.56	
P9	450	14.13	
P10	366	15.31	
P11	254	14.02	

**Table S9. Scavengers used, RSs quenched, and photocatalytic efficiency with quenched reactive species during the photocatalytic TC degradation process.**

Quencher	RSs	$k_{\text{obs}}$ ( $\text{min}^{-1}$ )	Photocatalytic efficiency
----------	-----	--	---------------------------

	Quenched		(%)
Blank(TC)	\	0.033	100
IPA	•OH	0.027	81.8
MeOH	h <sup>+</sup>	0.018	54.5
His	<sup>1</sup> O <sub>2</sub>	0.026	78.8
TEMPOL	O <sub>2</sub> <sup>•-</sup>	0.002	6.06
O <sub>2</sub>	\	0.0309	145.5
N <sub>2</sub>	O <sub>2</sub>	0.008	66.7

## Figures

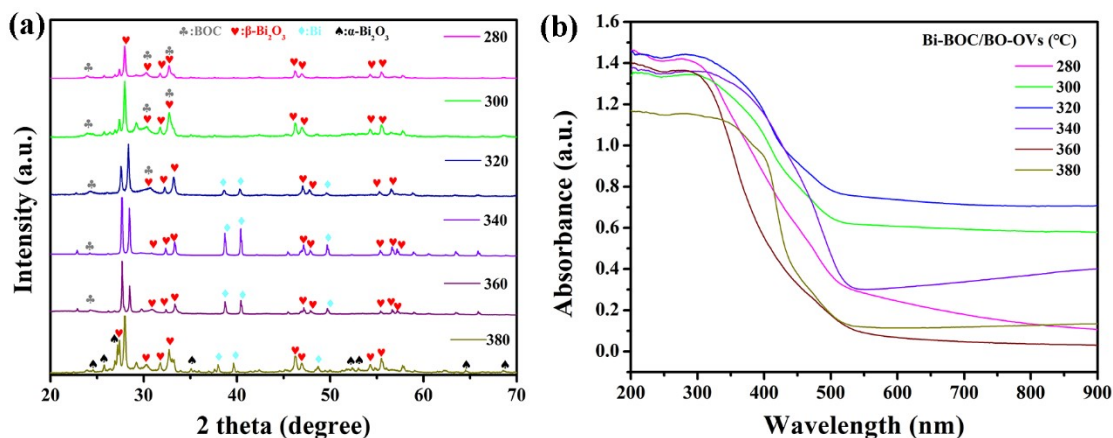


Fig S1. (a) XRD spectrum and (b) UV-vis DRS spectra of Bi-BOC/BO-OVs system calcined at different temperatures.

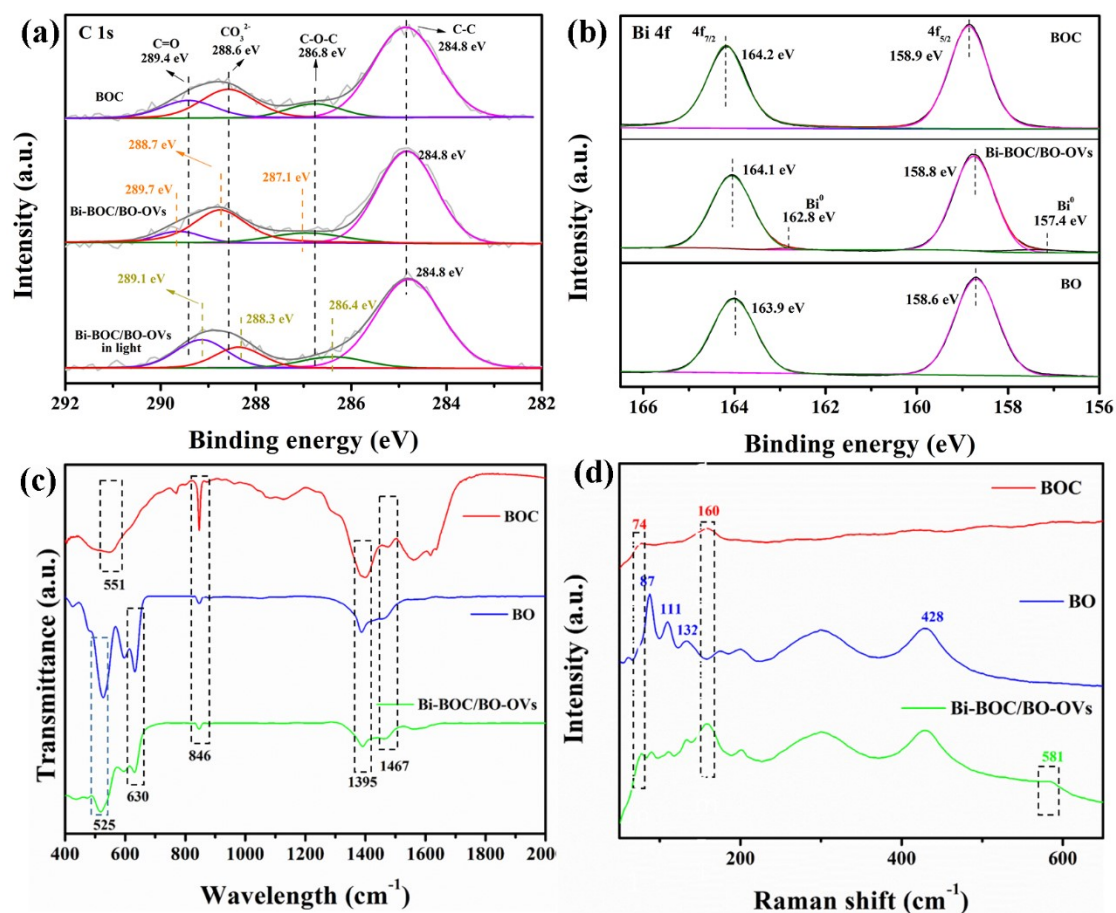




Fig. S2. (a) Ex-situ/ in-situ irradiated XPS spectra of C1s. (b) High-resolution XPS spectra of Bi 4f. (c) FT-IR spectrum and (d) Raman spectra of BOC, BO, and Bi-BOC/BO-OVs.

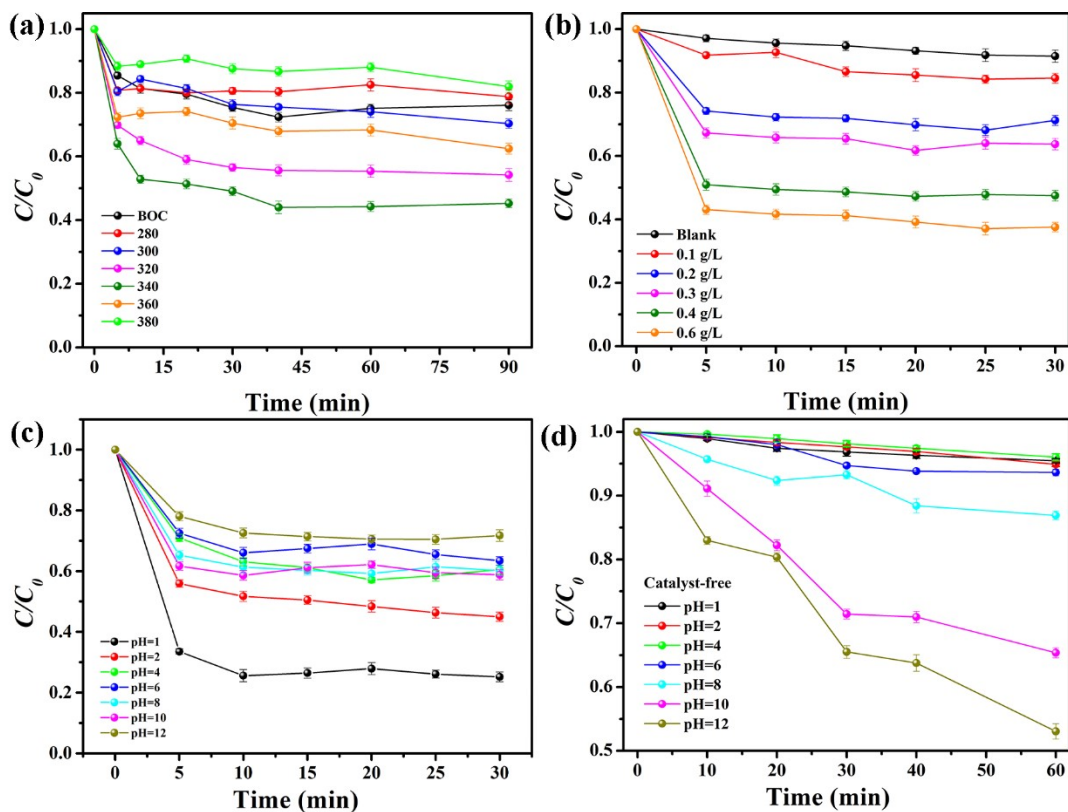
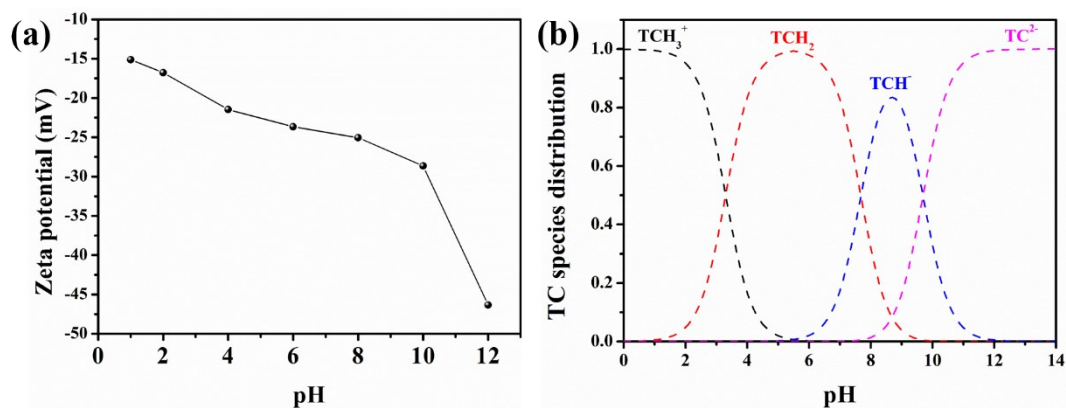
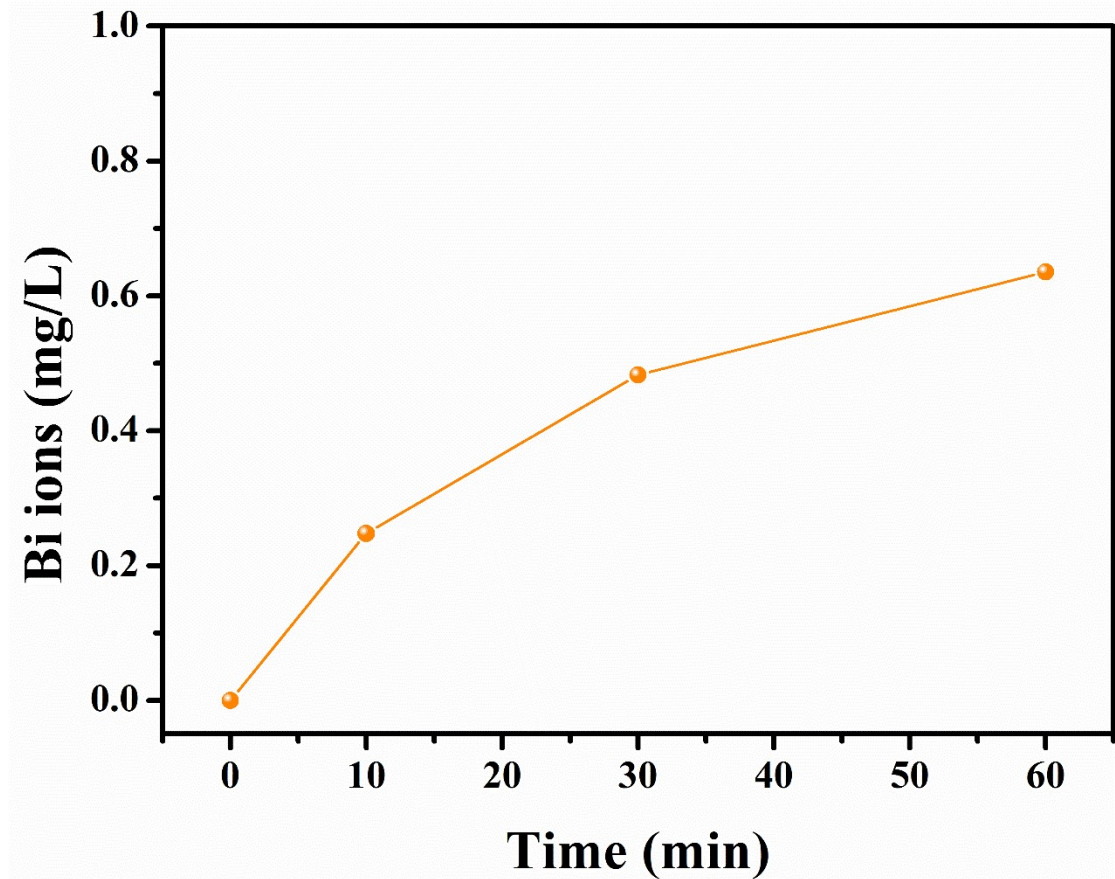


Fig S3. Adsorption for TC in the darkness of (a) different samples, (b) different photocatalyst concentrations and (c) different pH of Bi-BOC/BO-OVs. (d) Self-degradation of TC at different pH without catalyst.



---

**Fig S4. (a) Zeta potential of Bi-BOC/BO-OVs. (b) Species distribution of tetracycline under different pH.**



**Fig S5. Leakage of Bi ions in the Bi-BOC/BO-OVs system.**

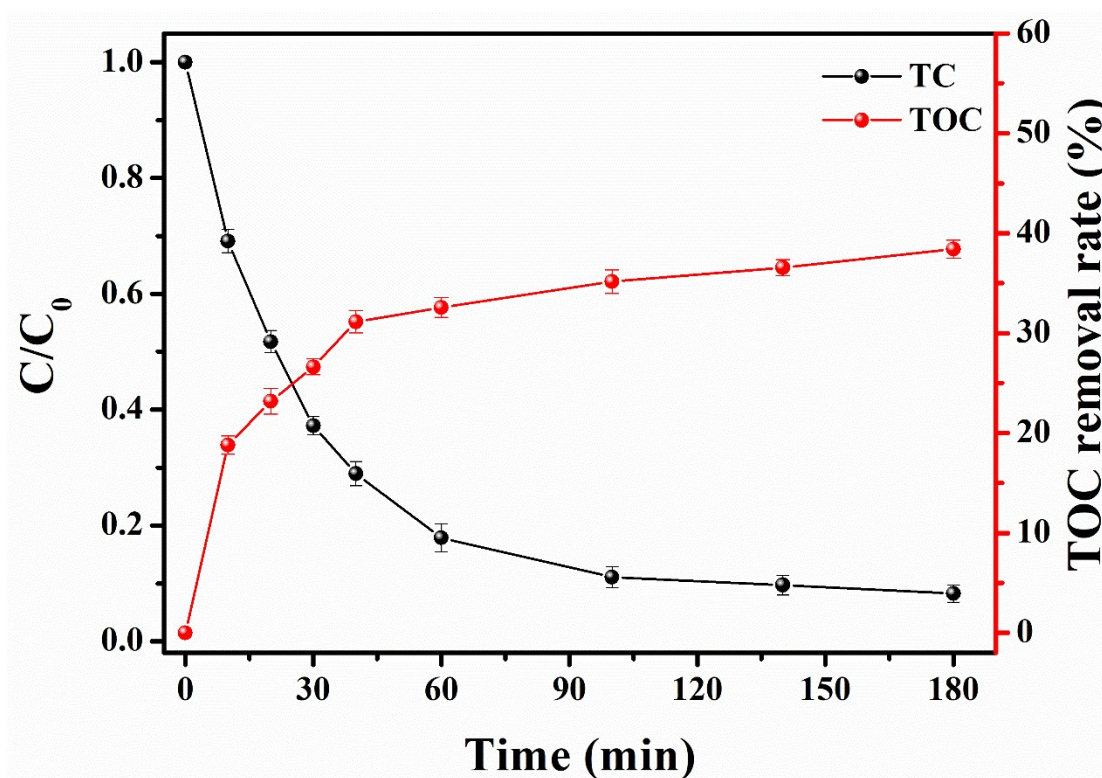
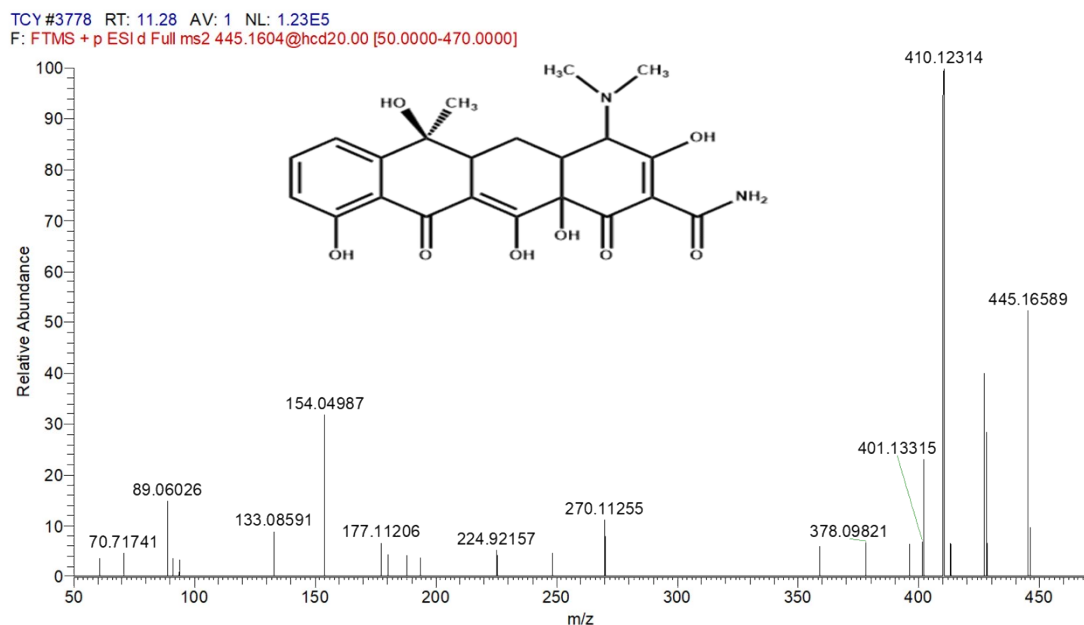
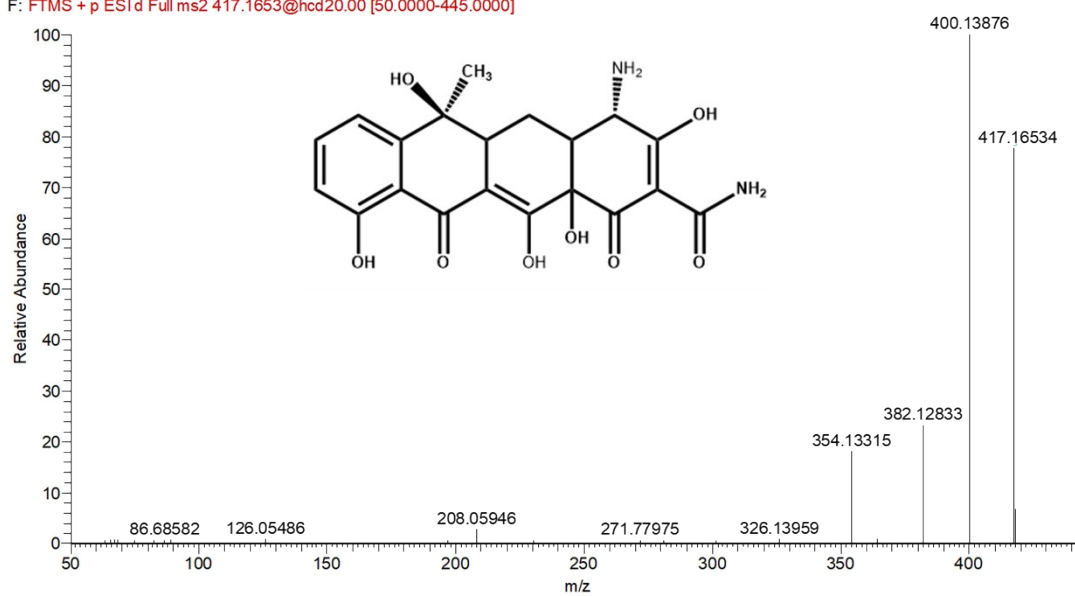


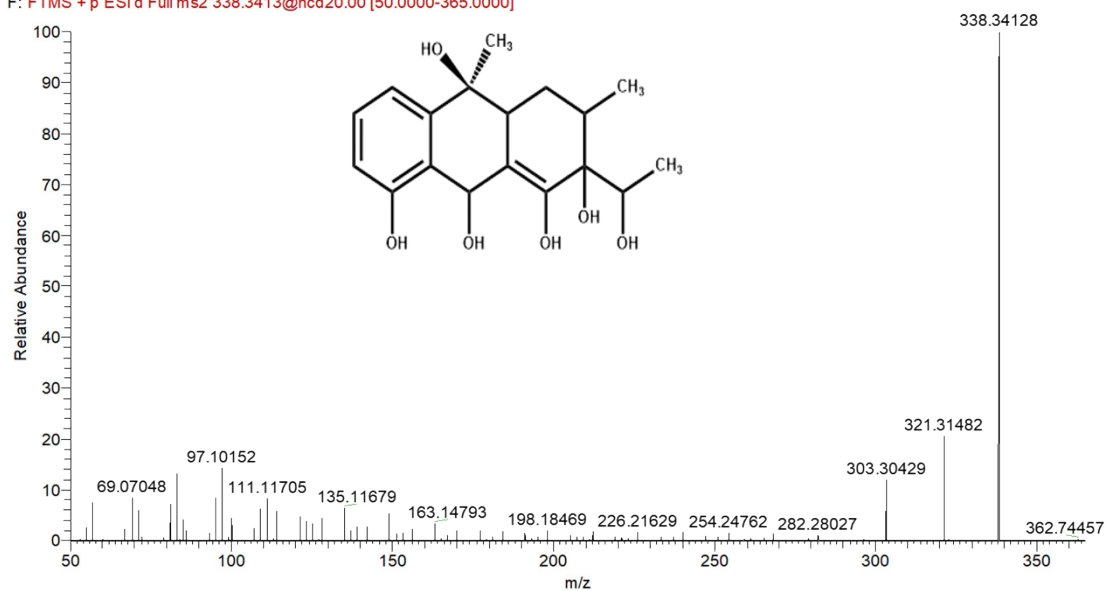
Fig S6. The mineralization of tetracycline during Bi-BOC/BO-OVs photocatalytic degradation process under visible light.



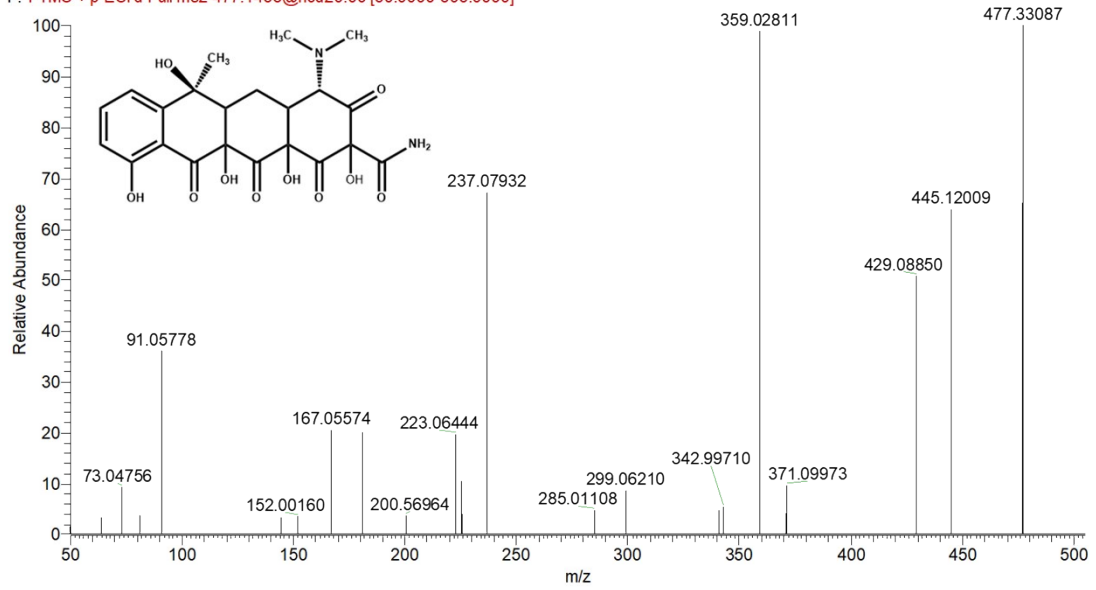
TCY #2854 RT: 8.53 AV: 1 NL: 6.59E5  
F: FTMS + p ESI d Full ms2 417.1653@hcd20.00 [50.0000-445.0000]



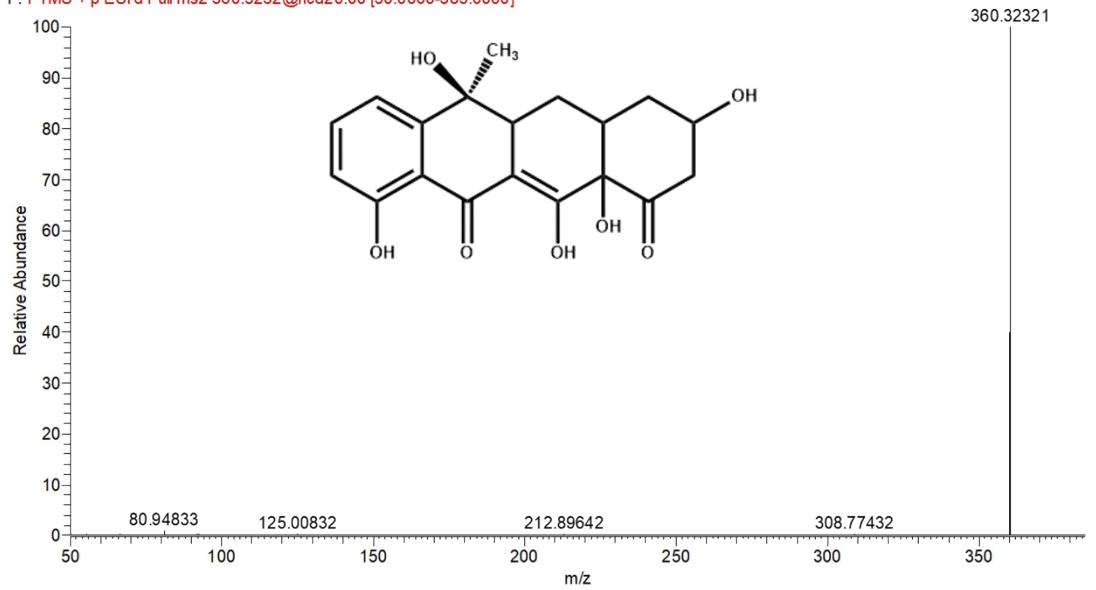
TCY #6274 RT: 18.72 AV: 1 NL: 3.24E6  
F: FTMS + p ESI d Full ms2 338.3413@hcd20.00 [50.0000-365.0000]



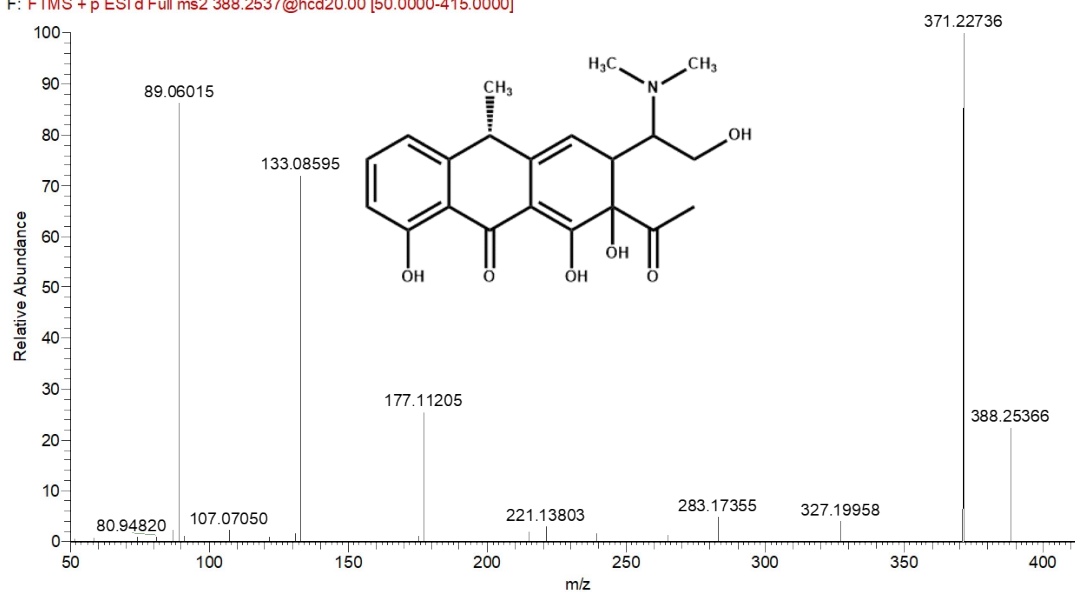
TCY #5998 RT: 17.89 AV: 1 NL: 1.33E5  
F: FTMS + p ESI d Full ms2 477.1456@hcd20.00 [50.0000-505.0000]



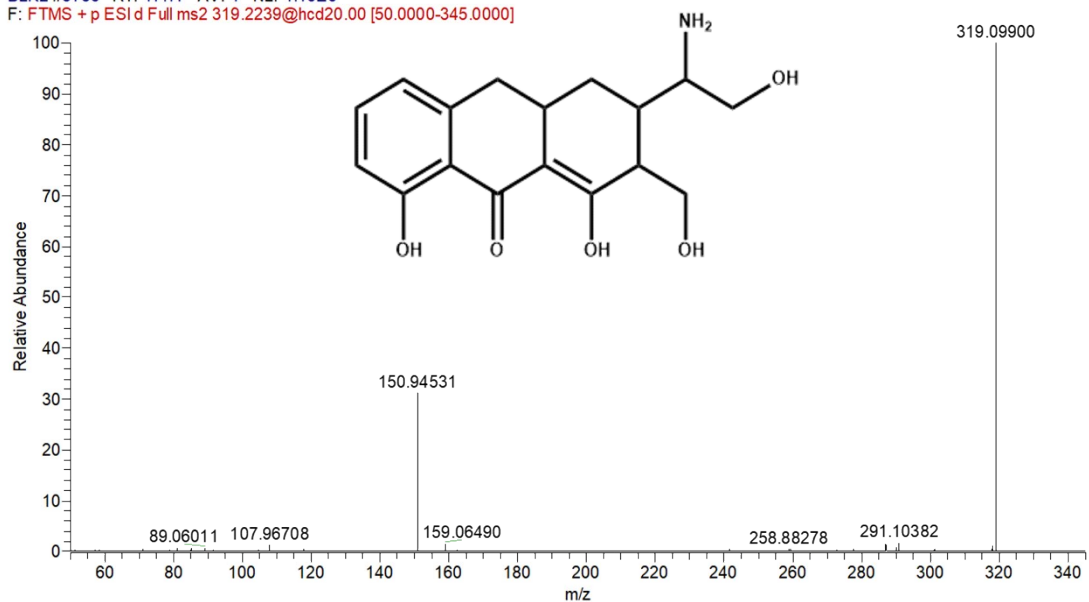
TCY #6264 RT: 18.69 AV: 1 NL: 1.26E6  
F: FTMS + p ESI d Full ms2 360.3232@hcd20.00 [50.0000-385.0000]



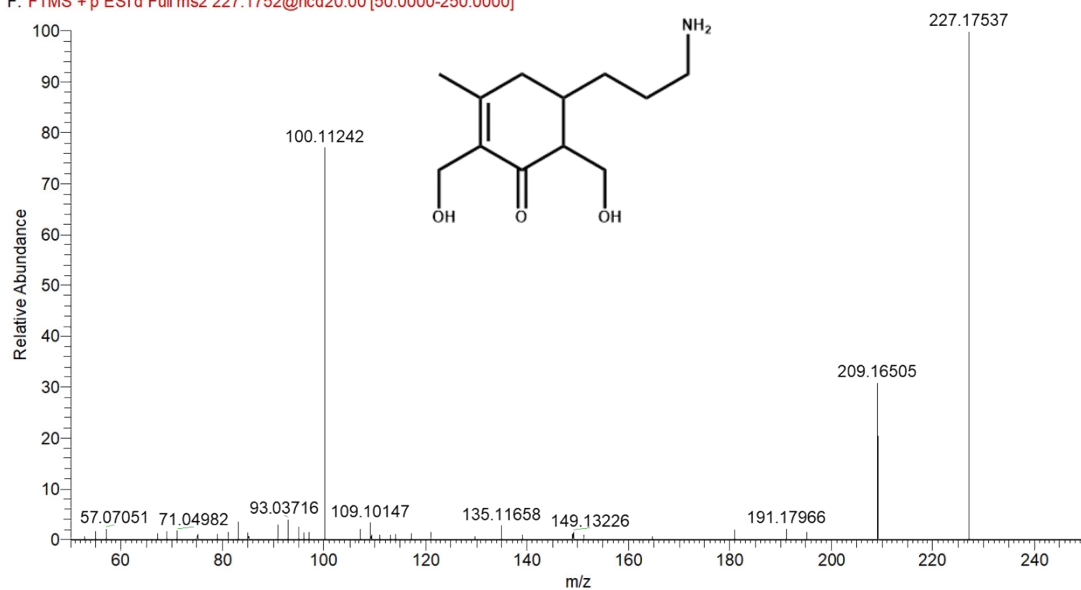
TCY #2952 RT: 8.82 AV: 1 NL: 5.31E5  
F: FTMS + p ESI d Full ms2 388.2537@hcd20.00 [50.0000-415.0000]



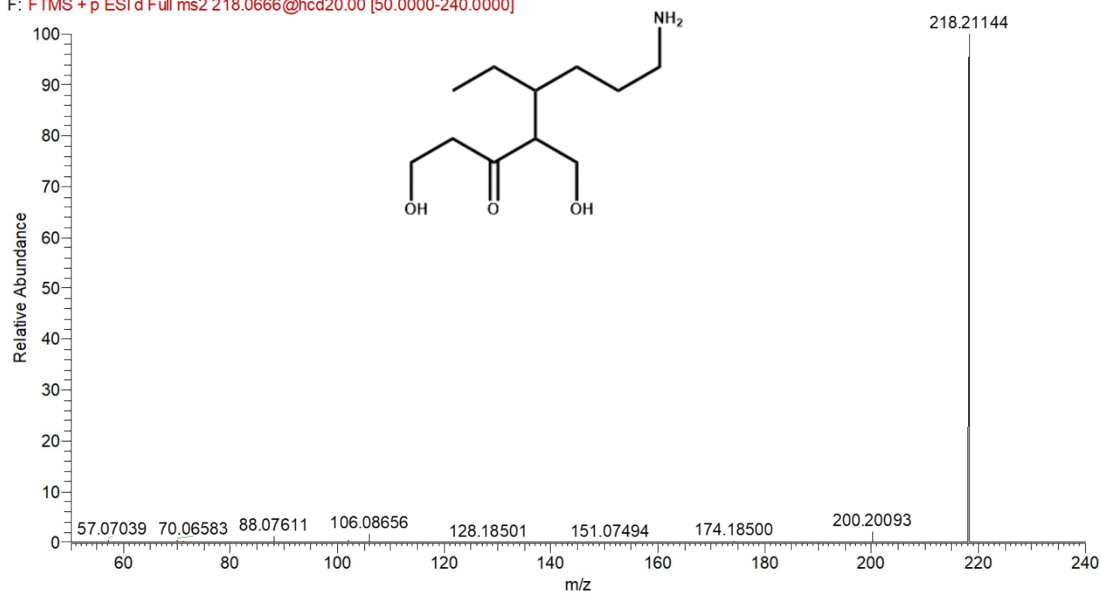
BLK2 #5756 RT: 17.17 AV: 1 NL: 1.16E6  
F: FTMS + p ESI d Full ms2 319.2239@hcd20.00 [50.0000-345.0000]



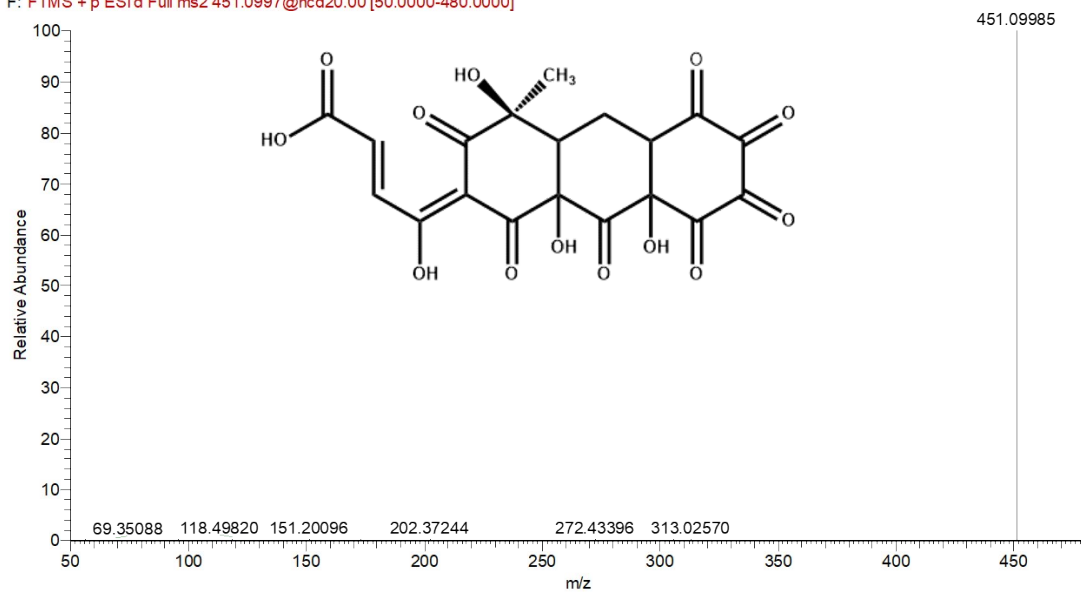
TCY #5074 RT: 15.13 AV: 1 NL: 4.40E5  
F: FTMS + p ESI d Full ms2 227.1752@hcd20.00 [50.0000-250.0000]



TCY #3536 RT: 10.56 AV: 1 NL: 4.35E6  
F: FTMS + p ESI d Full ms2 218.0666@hcd20.00 [50.0000-240.0000]



TCY #4738 RT: 14.13 AV: 1 NL: 2.34E6  
F: FTMS + p ESI d Full ms2 451.0997@hcd20.00 [50.0000-480.0000]



TCY #5134 RT: 15.31 AV: 1 NL: 1.61E6  
F: FTMS + p ESI d Full ms2 367.2087@hcd20.00 [50.0000-395.0000]

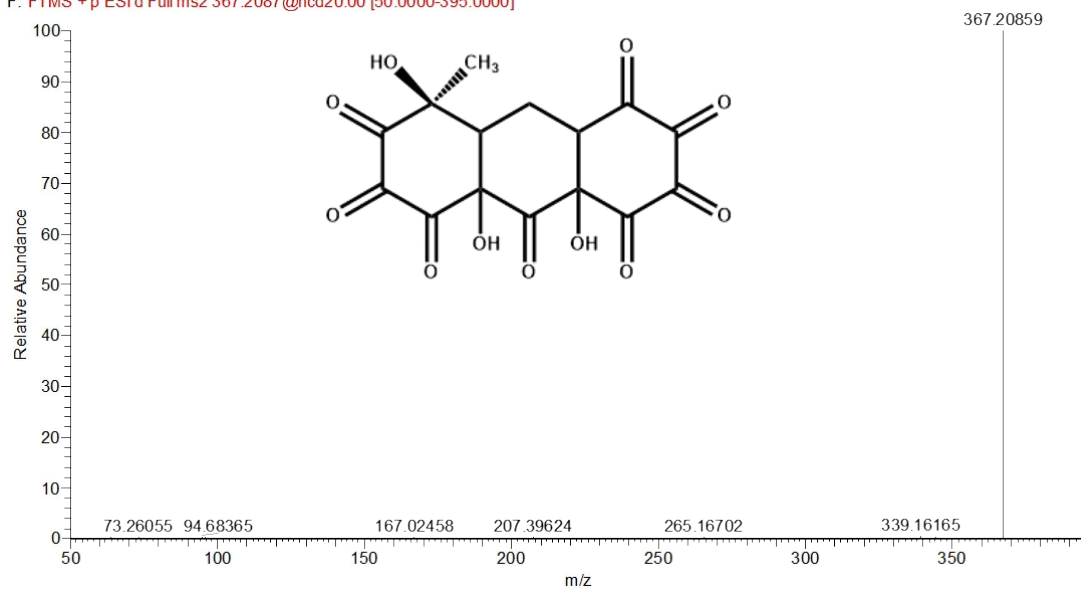


**Fig S7. Fragment chart analyses of the UHPLC-HRMS secondary ion mass spectrometry of the TC and its by-products.**



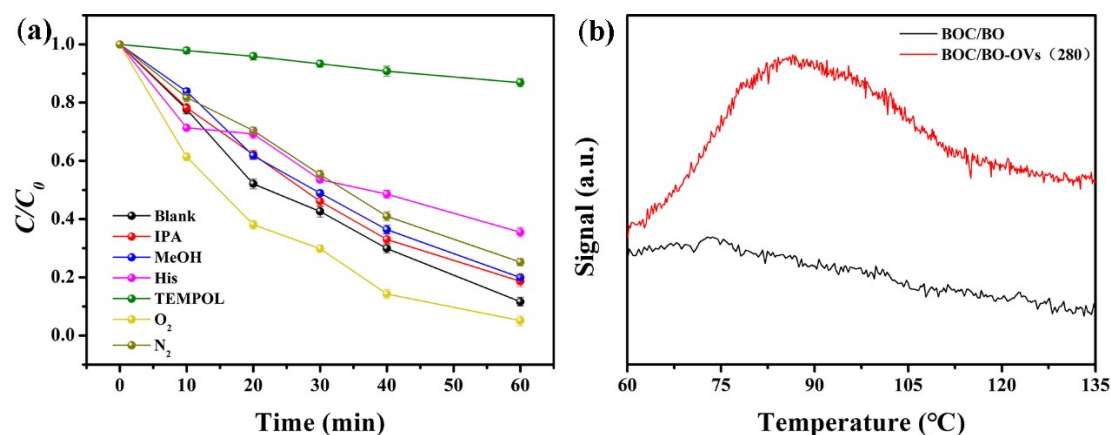


**Fig. S8. (a) Photocatalytic activity using different scavengers (TPA, MeOH = 3 mL, His=0.069 g, TEMPOL = 0.078 g). (b)  $O_2$ -TPD spectra of BOC/BO and Bi-BOC/BO-OVs.**

### Reference

1. X. Yang, Y. Wang, N. He, W. Wan, F. Zhang, B. Zhai and P. Zhang, One-step hydrothermal synthesis of hierarchical nanosheet-assembled  $Bi_2O_2CO_3$  microflowers with a  $\{001\}$  dominant facet and their superior photocatalytic performance, *Nanotechnology*, 2020, **31**, 375604.
2. P. Chen, H. Liu, Y. Sun, J. Li, W. Cui, L. a. Wang, W. Zhang, X. Yuan, Z. Wang, Y. Zhang and F. Dong, Bi metal prevents the deactivation of oxygen vacancies in  $Bi_2O_2CO_3$  for stable and efficient photocatalytic NO abatement, *Applied Catalysis B: Environmental*, 2020, **264**, 118545.
3. S. Yu, Y. Zhang, F. Dong, M. Li, T. Zhang and H. Huang, Readily achieving concentration-tunable oxygen vacancies in  $Bi_2O_2CO_3$ : Triple-functional role for efficient visible-light photocatalytic redox performance, *Applied Catalysis B: Environmental*, 2018, **226**, 441-450.
4. W. Hou, H. Xu, Y. Cai, Z. Zou, D. Li and D. Xia, Precisely control interface OV's concentration for enhance 0D/2D  $Bi_2O_2CO_3/BiOCl$  photocatalytic performance, *Applied Surface Science*, 2020, **530**, 147218.
5. C. Lai, F. Xu, M. Zhang, B. Li, S. Liu, H. Yi, L. Li, L. Qin, X. Liu, Y. Fu, N. An, H. Yang, X. Huo, X. Yang and H. Yan, Facile synthesis of  $CeO_2$ /carbonate doped  $Bi_2O_2CO_3$  Z-scheme heterojunction for improved visible-light photocatalytic performance: Photodegradation of tetracycline and photocatalytic mechanism, *Journal of Colloid and Interface Science*, 2021, **588**, 283-294.
6. H. Zhou, S. Zhong, M. Shen and Y. Yao, Composite soft template-assisted construction of a flower-like  $\beta-Bi_2O_3/Bi_2O_2CO_3$  heterojunction photocatalyst for the enhanced simulated sunlight photocatalytic degradation of tetracycline, *Ceramics International*, 2019, **45**, 15036-15047.
7. H. Zhao, G. Li, F. Tian, Q. Jia, Y. Liu and R. Chen, g-C $_3$ N $_4$

---

surface-decorated Bi<sub>2</sub>O<sub>2</sub>CO<sub>3</sub> for improved photocatalytic performance: Theoretical calculation and photodegradation of antibiotics in actual water matrix, *Chemical Engineering Journal*, 2019, **366**, 468-479.

8. S. Li, S. Hu, W. Jiang, Y. Liu, Y. Liu, Y. Zhou, L. Mo and J. Liu, Ag<sub>3</sub>VO<sub>4</sub> Nanoparticles Decorated Bi<sub>2</sub>O<sub>2</sub>CO<sub>3</sub> Micro-Flowers: An Efficient Visible-Light-Driven Photocatalyst for the Removal of Toxic Contaminants, *Frontiers in Chemistry*, 2018, **6**.